RESEARCH PAPER

The Effect of B Addition on the Structure and Magnetic Properties of AlCrFeNiMnSi, a High Entropy Alloy

Ehsan Tarighati, Majid Tavoosi*, Ali Ghasemi, Gholam Reza Gordani

* ma.tavoosi@gmail.com
Department of Materials Engineering, Malek-Ashtar University of Technology, Iran.

Abstract: *In the present study, the effect of boron on the structural and magnetic properties of AlCrFeNiMnSiBx high entropy alloys (HEAs) were investigated. In this regard, different percentage of boron element was added to the base composition and the samples were characterized using X-ray diffraction (XRD), scanning electron microscopy (SEM) and vibrating sample magnetometer (VSM) methods. Based upon the results obtained, the tendency of Si element for the formation of silicide phases prevents the stabilization of single FCC and BCC solid solution phases in AlCrFeNiMnSi alloy. The boron element has significant effect on destabilization of silicide phases and by increasing in the percentage of this element, the simple BCC solid solution phase was observed to be the dominate phase. Of course, the presence of boron had an adverse effect on the magnetic properties of prepared alloys. The magnetization saturation of AlCrFeNiMnSiBx decreased from 29.8 to about 6 emu/g with the increase in the boron content.*

Keywords: High entropy alloy, Magnetic properties, Mechanical alloying, Annealing.

1. INTRODUCTION

High entropy alloy (introduced by Yeh et al. [1] in 2004) has attracted much attention due to unique properties such as high strength and hardness, good wear resistance, and excellent thermal stability. These alloys are the solid solutions with at least 5 principle elements with the almost equal atomic ratio vary from 5 to 35% [2-7]. The high mixing entropy in these alloys makes solid solution phase more stable than intermetallic compounds and other complex phases.

Since, most HEAs contain of ferromagnetic metallic elements, the magnetic characteristics of these alloys attracted great attention to the researchers [1-3]. Same as other physical and mechanical properties, the magnetic properties of these alloys are highly sensitive to the additional elements. For example, it has been shown that, the Al element can change the magnetic behavior of FeCoCrNi alloy from paramagnetic to ferromagnetic through a FCC to BCC phase transformation. The Nb, W and Zr element has destructive effect on magnetic behaviors of CoFeNi HEAs as a result of the formation of paramagnetic phases. The Bi has been reported as a promotion for soft-to-hard ferromagnetic transition in the equiatomic FeCoNiMn HEAs [12] and Cu has negligible effect on magnetic behaviors of AlCoCrCuFeNi alloy.

Besides that, the effects of B and Si elements on structural and magnetic behaviors of different HEAs were investigated. For instance, Zeo et al. [11] report that Si has destructive effect on magnetic properties of CoFeNi based alloys due to the formation of Ni_3Si and other silicide phases in the microstructure [11]. Moreover, based on Xu [12] and Qiushi at al. [13] studies, B and Si elements have negative effects on magnetic characteristics of FeSiBAlNi and AlCoCrFeNiBx alloys due to the tendency for the formation of silicide and boride phases.

Although, there are a lot of publication about the formation and characterization of different HEAs [1-13], the exact effect of alloying elements on structural and magnetic properties of these alloys have not been properly investigated. However, the present work focuses on the effect of boron addition on structural and magnetic characteristics of AlCrFeNiMnSiBx high entropy alloys.

2. EXPERIMENTAL PROCEDURE

High purity Fe, Ni, Mn, Cr, Al, Si and B powders were used as raw materials (Table 1). Four powders mixture of initial elements, based on AlCrFeNiMnSiBx (x= 0, 0.5, 0.75 and 1) composition (at. %), were mechanically milled in a planetary ball mill in an argon atmosphere (the

Ehsan Tarighati, Majid Tavoosi, Ali Ghasemi, Gholam Reza Gordani

rotation speed of 400 rpm and the ball to powder ratio of 10:1). Annealing procedure had been done at temperature of 900ºC for 2 h followed with quenching in cold water. Before annealing, the powder samples were sealed in a quartz tube under the vacuum of 10^{-3} Pa in order to prevent form oxidation during annealing.

XRD technique, using a diffractometer with Cu Ka radiation (λ= 0.15406 nm; 40 kV; Philips PW3710) was used to follow the structural changes of the specimens (step size: 0.05°; time per step: 1s). Morphological characterization of as-milled and annealed samples was carried out by scanning electron microscopy (VEGA-TESCAN-XMU) at an accelerating voltage of 20 kV. Magnetic properties (saturation magnetization and approximate coercivity) of produced samples were also measured using vibrating sample magnetometer (VSM) under an applied field up to 10 kOe.

3. RESULTS AND DISCUSSION

The XRD patterns of AlCrFeNiMnSiBx (x=0, 0.5, 0.75 and 1) alloys after 10 h of milling are presented in Fig. 1. The XRD analysis reveals that the elemental mixture contains peaks correspond to the constituent elements. Of course, boron is not detected by XRD because it is in amorphous state. As seen, there is not any evidence of formation of solid solution phases or other chemical compounds in specimens. In other words, the formation of homogenous physical mixture of the precursors is the final result from milling process. The presented SEM micrographs in Fig. 2 also confirm this point. However, this result is not in agreement with other reports about the formation of simple solid solution phases during milling process in Co-Ni, Fe-Co-Ni and Fe-Ni systems [12].

During ball milling process, the present element in the vial are subjected to high impact force which lead to fragmentation of brittle materials and flattening of ductile materials. Moreover, the milling process involved repeated cold welding,

fracturing and re-welding which forms homogeneous-single/multi solid solution of powders. In fact, the difference in used milling parameters such as rotation speed, ball to powder ratio, the size and distribution of balls, milling atmosphere, temperature and time in this work in comparison with others is the main reason of this discrepancy.
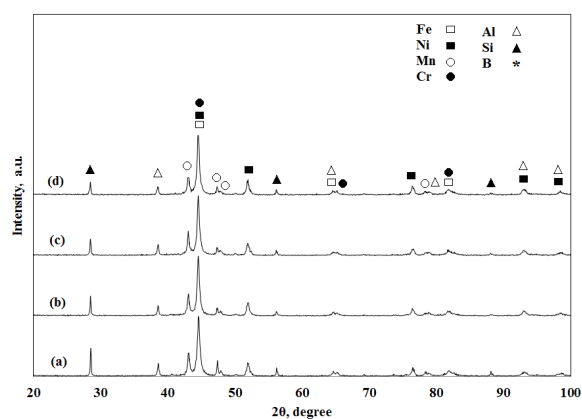

Fig. 1. The XRD patterns of AlCrFeNiMnSiBx as-milled powder mixtures, a) x= 0, b) x= 0.5, c) x= 0.75 and d) x= 1.

The XRD patterns and SEM micrographs of milled samples after annealing process at 900°C for 2 h are presented in Figs. 3 and 4, respectively. Figure 3 (a) details the XRD pattern of B-0 alloy. When comparing this alloy with traditional HEAs with BCC and/or FCC phases, it is surprising to find them to be more complex. The ordered Cr_5Si_3, $FeNi_3$, Fe_2Si and Ni_2Si phases, along with a solid solution phase, are observed in the diffraction graph of this alloy.

The non-uniform distributions of alloying elements in this sample after annealing process, which are presented in Fig.5, also confirm this point. In this study, the intensity of the diffraction peak of the ordered intermetallic phase is considered as the strongest and is obviously higher than the peaks of the solid solution phases, which indicate that the intermetallic phases are the dominant.

Table 1. The purity and producing company of used raw materials in this study.

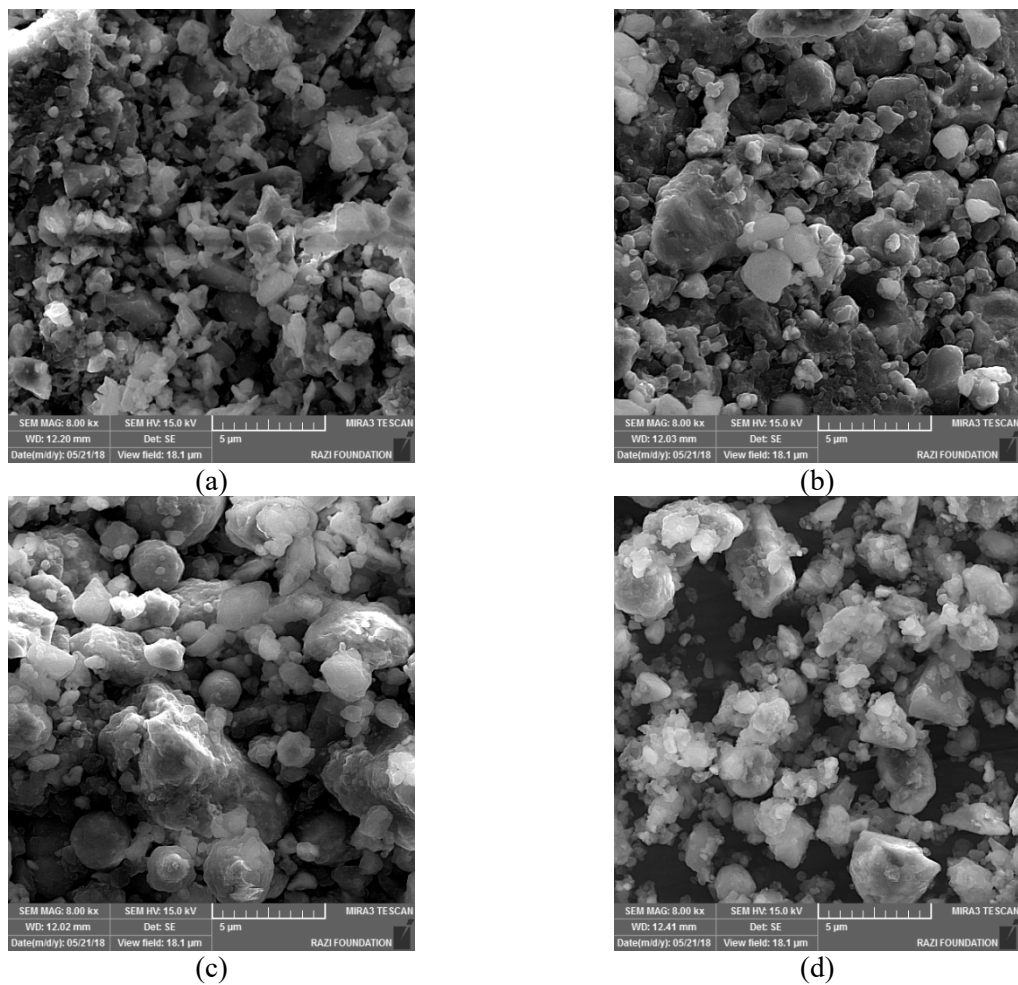|	**Fe**	**Ni**	**Mn**	**Cr**	**Al**	**Si**	**B**
Company	Merck (103819)	Merck (112277)	Merck (112237)	Merck (112097)	Merck (101056)	Merck (112497)	Merck (112070)
Purity (%)	99	99.9	99.9	99.9	99.9	99	99

(a)

(b)

(c)

(d)

Fig. 2. The SEM micrographs of AlCrFeNiMnSiBx powder mixture after 10 h of milling process, a) x= 0, b) x= 0.5, c) x= 0.75 and d) x= 1.
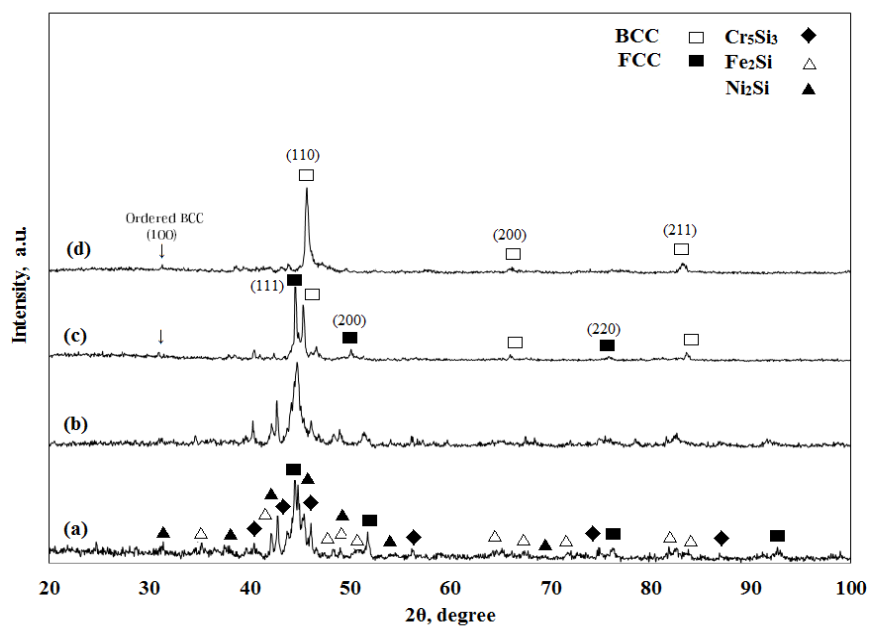

Fig. 3. The XRD patterns of AlCrFeNiMnSiBx milled powder mixture after annealing process, a) x= 0, b) x= 0.5, c) x= 0.75 and d) x=1.
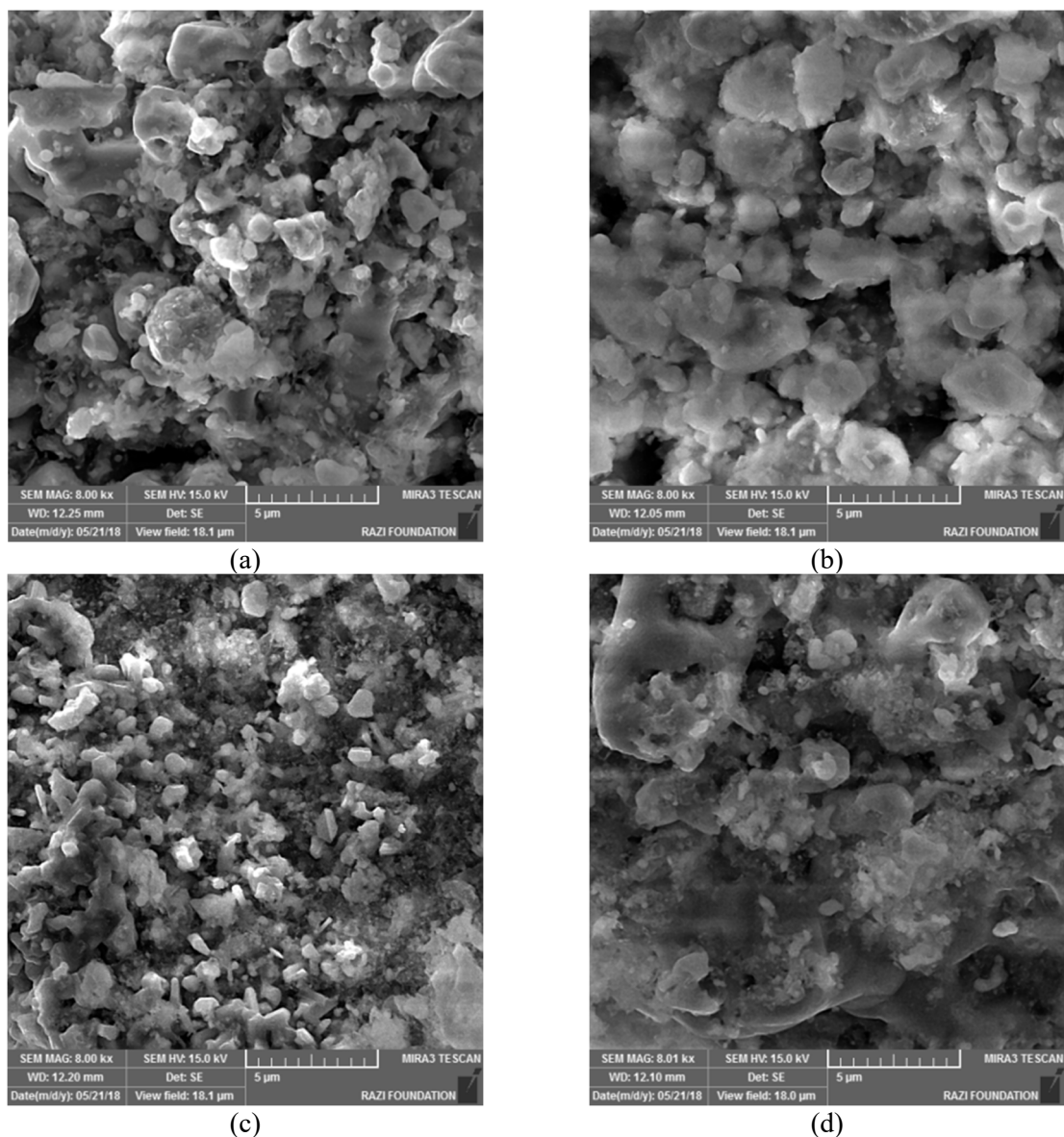
(a)

(b)

(c)

(d)

Fig. 4. The SEM micrographs of AlCrFeNiMnSiBx milled powder mixture after annealing process, a) x= 0, b) x= 0.5, c) x= 0.75 and d) x= 1.

Based on presented XRD pattern in Fig. 3(b), the structure of B-0.5 alloy is similar to the B-0 and composed of solid solution and order Cr_5Si_3, $FeNi_3$, Fe_2Si and Ni_2Si intermetallic phases. However, the intensities of ordered phases are weaker than those detailed in Fig. 3(a), which suggest that the volume fraction of the ordered phases has been decreased. In contrast to B-0 and B-0.5 samples, B-0.75 and B-1 alloys exhibit duplex FCC+BCC and single BCC phase, respectively. Furthermore, the diffraction peak for ordered BCC (100) phase could be detected in these two alloys. It is apparent that the B acts as a BCC former in AlCrFeNiMnSiBx alloy due to the transition of crystal structure from multi-complex phases to a single BCC phase. The lattice parameter of BCC phase with the best fit of XRD peaks is found to be 2.875 A°. The uniform distributions of prepared alloying elements of AlCrFeNiMnSiB alloy which are presented in Fig. 6 also confirm the formation of single phase solid solution in this sample. Different experimental studies confirmed that the formation of simple solid solution phase depends on the value of enthalpy of mixing (ΔH_{mix}), entropy of mixing (ΔS_{mix}), and difference in atomic size (δ) of constituent elements. These parameters are defined as following equations [3] and the results are presented in Table 2.

Fig. 5. The elemental maps of different alloying elements in AlCrFeNiMnSi sample after annealing process, a) Al, b) Cr, c) Fe, d) Ni, e) Mn and f) Si.
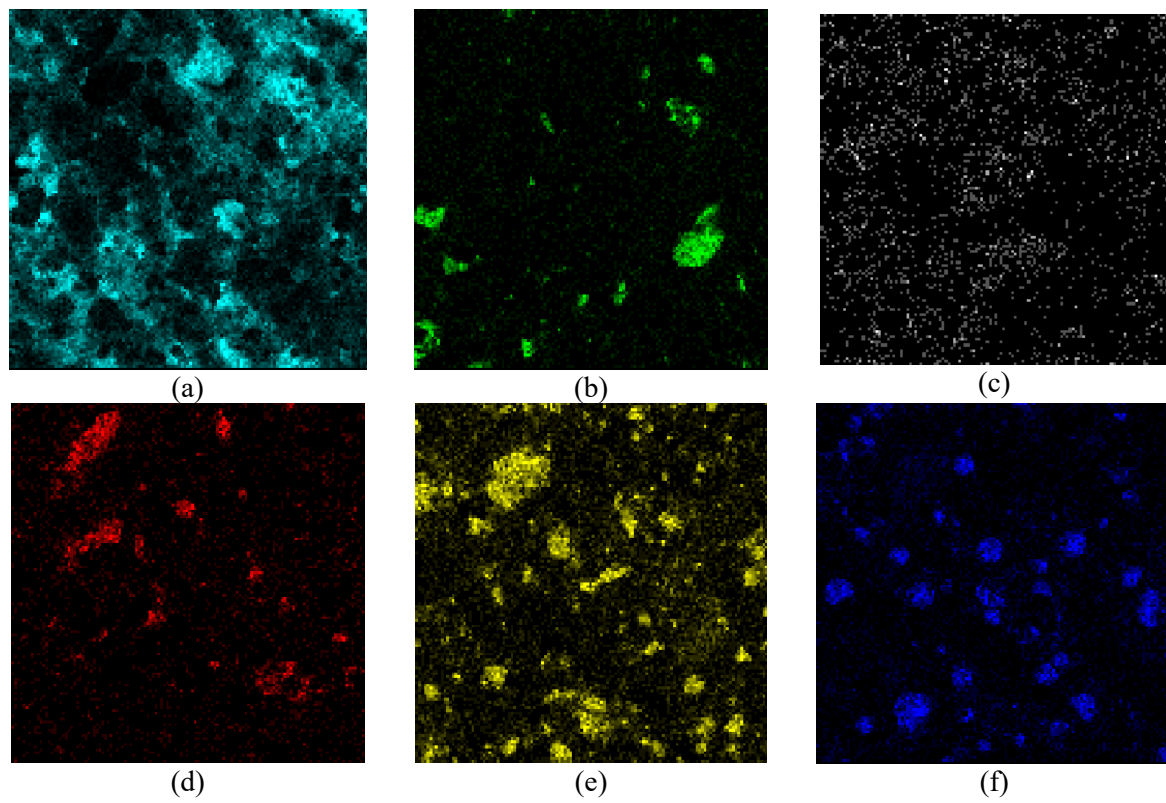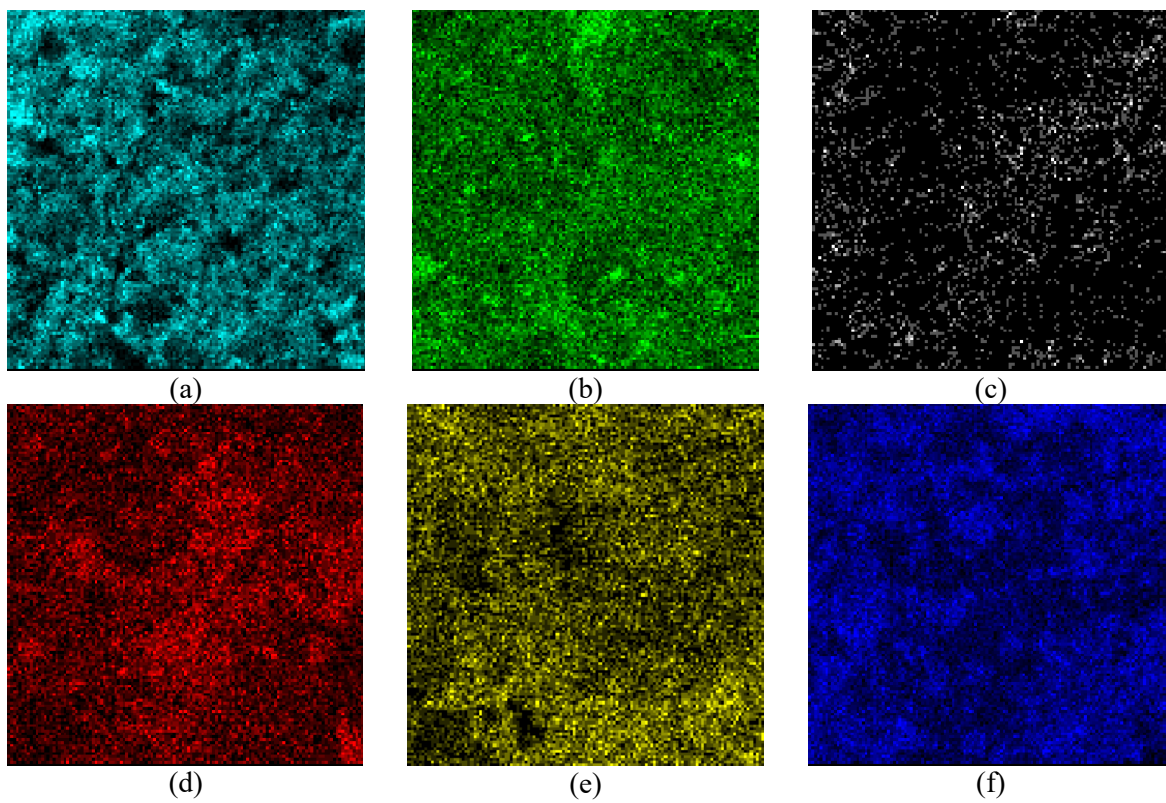

Fig. 6. The elemental maps of different alloying elements in AlCrFeNiMnSiB sample after annealing process, a) Al, b) Cr, c) Fe, d) Ni, e) Mn and f) Si.

Ehsan Tarighati, Majid Tavoosi, Ali Ghasemi, Gholam Reza Gordani

Table 2. Topological and thermodynamic parameters of AlCrFeNiMnSiBx alloying system.

Sample	δ (%)	ΔH_{mix} (KJ/mol)	ΔS_{mix} (J/mol.K)
AlCrFeMnNiSi	4.9	-28.33	1.79R
AlCrFeMnNiSiB$_{0.5}$	8.53	-28.34	1.93R
AlCrFeMnNiSiB$_{0.75}$	9.35	-29.06	1.94R
AlCrFeMnNiSiB	10.06	-31.18	1.95R

$$\Delta S_{mix} = -R \sum_{i=1}^{n} c_i ln c_i \qquad (1)$$

$$\Delta H_{mix} = \sum_{i=1, j>i}^{n} 4\Delta H_{AB}^{mix} c_i c_j \qquad (2)$$

$$\delta = \sqrt{\sum_{i=1}^{N} c_i \left(1 - r_i / \sum_{j=1}^{n} c_j r_j\right)^2} \qquad (3)$$

where R is the gas constant, n is the number of alloying elements and ci is the atomic percentage for the ith element and ΔH_{ABmix} is the enthalpy of mixing for the binary equiatomic AB alloys. The r_i or r_j is also the atomic radius for the ith or jth component. Based on literature, the primary preconditions for the formation of a solid solution in the HEAs are; - 22≤ ΔH_{mix} ≤7 kJ/mol, δ≤8.5% and 11≤ΔS_{mix}≤19.5 J/K.mol [3].

As seen, beside the ΔS_{mix}, other presented parameters could not satisfy the criteria for the formation of simple solid solution phase in AlCrFeNiMnSiBx system. In this regards, the formation of simple solid solution phases in B-0.75 and B-1 samples can be related to the beneficial effects of boron on the stabilization of simple solid solution phases in AlCrFeNiMnSi HEA as follow: (a) boron has negative enthalpy of mixing with all other selected elements presents in AlCrFeNiMnSi, due to which formation of solid solution phase enhances, (b) boron has small atomic radius than Fe, Ni, Cr, Al, Si and Mn, the size difference leads the lattice distortion in the alloy system that impedes the ability of formation of simple solid solution phases, (c) the addition of boron as an extra element for the case of HEA can increase cofigurational entropy of mixing of the system and promotes the formation of a solid solution phase rather than the precipitation of intermetallic phases. The SEM micrographs of milled samples after annealing process at 900°C for 2 h are presented in Fig. 4. The annealed sample has the granular morphology size ranging from 1 to 14 μm. Increase in particle size is observed after the annealing, which is due to the grain growth phenomenon of the synthesized HEA. EDX analysis has been performed through the selection of five different regions for recording the EDX

spectra and found that the synthesized HEA exhibit good chemical homogeneity.

To study about the effect of boron content on magnetic properties of the AlCrFeMnNiSiB$_x$ HEAs, the hysteresis loops of the milled and vacuum annealed samples measured at room temperature through the VSM are presented in Fig. 7. By attention to this point, several points can be concluded as:

-   All milled and annealed samples exhibit ferromagnetic characteristics.
-   The saturation of magnetization and coercive force of milled samples in different composition are in the range of 56-57 emu/g and 60-70 Oe, respectively. As seen, there is no significant difference between presented magnetic characteristics. In fact, relatively same compositional, structural and topological characteristics of milled sample (based on Figs. 1 and 2) are the main reason of this manner.
-   Annealing process has significant effects on magnetic properties of milled samples. Based on Fig. 7, during annealing process, the saturation of magnetization decreases form 56-57 emu/g to about 8-29.8 emu/g. Hence the separation between the ferromagnetic elements of HEAs increased after annealing due to the formation of intermetallic compounds such as Cr_5Si_3, $FeNi_3$, Fe_2Si and Ni_2Si, the magnetic exchange coupling is altered and the value of Ms decreased for annealed samples.
-   As the content of boron increased, the Ms value decreases from 29 to about 6 emu/g. Based on literature, the magnetic behavior of the HEAs highly depends on the base alloy, addition of elements and the resultant crystal structure formed after mutual interaction between the alloying elements [21-26]. Based on above, as the content of boron increased, the structure of the alloy changed from a multi-complex structure of FCC solid solution and order intermetallic phases to a mixture of FCC and BCC and then it transformed into a single BCC phase.
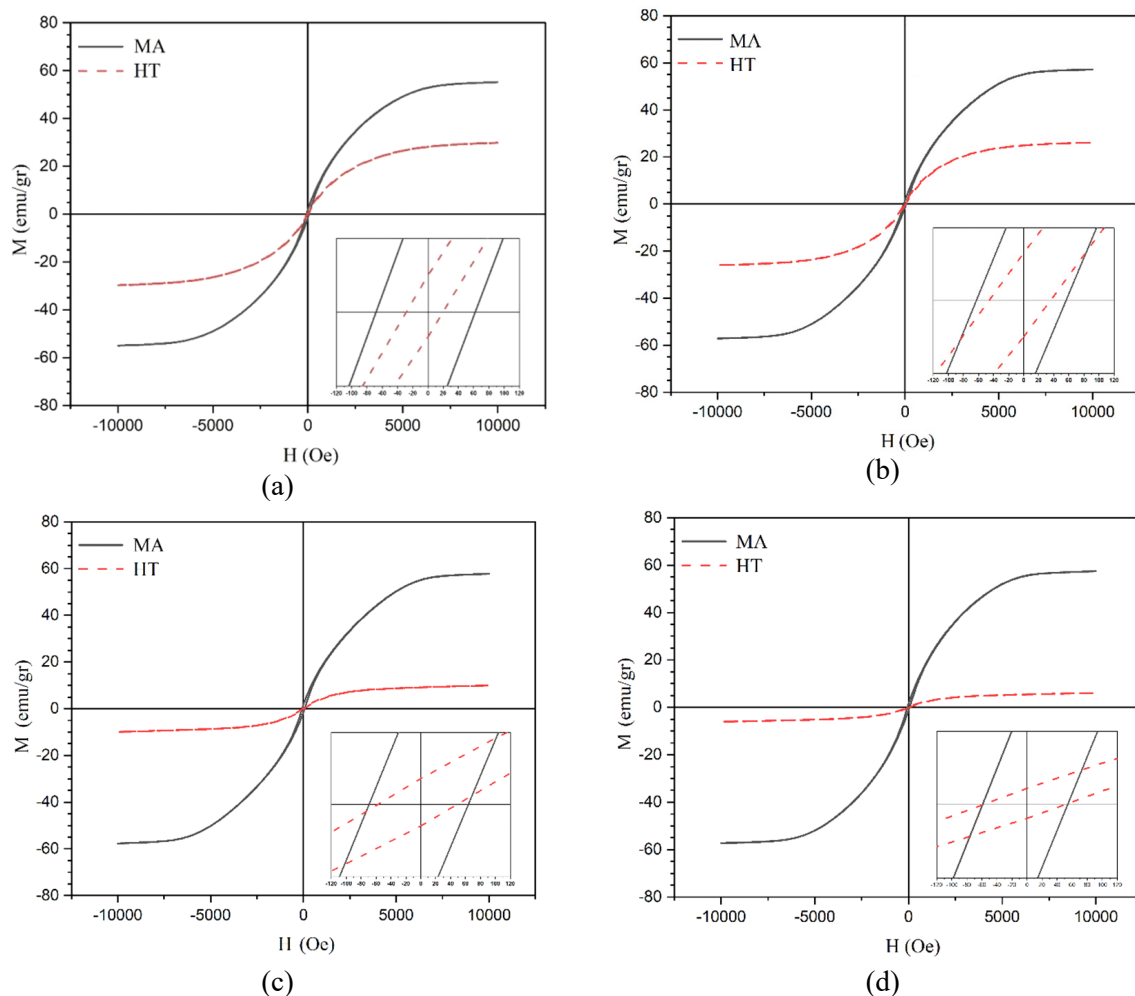
6

Fig. 7. Magnetic hysteresis loops of AlCrFeNiMnSiBx milled powder mixture before and after annealing process, a) x= 0, b) x= 0.5, c) x= 0.75 and d) x= 1.

By attention to the presented results in literature, it was expected that, AlCrFeMnNiSiB alloy with single BCC solid solution structure must show the best magnetic characteristics. However, experimental finding shows that, the Ms value of this alloy is the lowest. In fact, the enhanced magnetic characteristics of AlCrFeMnNiSi alloy only can be related to the percentage of ferromagnetic elements in composition. In fact, AlCrFeMnNiSi HEA having 33.33 at.% of ferromagnetic elements, while AlCrFeMnNiSiB having 28.57 at.% of ferromagnetic elements. By attention to this point, the Ms value of AlCrFeMnNiSi HEA is higher than AlCrFeMnNiSiB$_x$ alloys.

The values of saturation magnetization and coercive force of AlCrFeNiMnSi HEA are found to be 29.8 emu/g and 58 Oe, respectively. This sample shows better magnetization as compared to some recently reported HEAs. This value of magnetization is higher than the reported CoCrFeNiMn (1.34 emu/g), CoCrFeNiTiAl0.5/2.0 (2.48-0.76 emu/g), FeCoCrNi (3 emu/g), CoCrFeNiCuTix (0.3-1.55 emu/g) and Al$_2$CrFeNiCoCuTi (1.2 emu/g) HEAs [25-28].

4. CONCLUSIONS

An investigation about the effect of boron content on the structural and magnetic properties of FeNiMnCrAlSiB$_x$ HEAs was the main goal of this work. Based upon results obtained, the constituent phases in the AlCrFeNiMnSi alloy were composed of ordered Cr$_5$Si$_3$, FeNi$_3$, Fe$_2$Si and Ni$_2$Si, along with a solid solution phase. The boron had a significant effect on destabilization of

intermetallic phases. With the increase in the percentage of this element, the simple BCC phase solid solution was the dominate phase in FeNiMnCrAlSiB sample. Boron had an adeverse effect on magnetic properties of FeNiMnCrAlSiB$_x$ HEAs. The magnetization saturation decreased from 29.8 to about 6 emu/g with the increase in the boron content.

REFERENCES

[1] Yeh, J.W., Chen, S.K., Lin, S.J., Gan, J.Y., Chin, T.S., "Nanostructured high-entropy alloys with multiple principal elements: Novel alloy design concepts and outcomes", Adv. Eng. Mater., 2004, 6-5, 299-303.

[2] Zhang, Y., Zuo, T.T., Tang, Z., Gao, M.C., Dahmen, K.A., "Microstructures and properties of high-entropy alloys", Prog. Mater. Sci., 2014, 61, 1-93.

[3] Zhang, Y., Zhou, Y.J., Lin, J.P., Chen, G.L., Liaw, P.K., "Solid-Solution phase formation rules for multi-component alloys", Adv. Eng. Mater., 2008, 10, 534-538.

[4] Tong, C.J., Chen, M.R., Yeh, J.W., Lin, S.J., Chen S.K., "Mechanical performance of the Al$_x$CoCrCuFeNi high-entropy alloy system with multiprincipal elements", Metall. Mater. Trans., 2005, 36, 1263-1271.

[5] Lin, C.M., Tsai, H.L., Bor, H.Y., "Effect of aging treatment on microstructure and properties of high-entropy Cu$_{0.5}$CoCrFeNi alloy", Intermetallics, 2010, 18, 1244-1250.

[6] He, J.Y., Liu, W.H., Wang, H., Wu, Y., Liu, X.J., "Effects of Al addition on structural evolution and tensile properties of the FeCoNiCrMn high-entropy alloy system", Acta Mater., 2014, 62, 105-113.

[7] Chou, H.P., Chang, Y.S., Chen, S.K., Yeh, J.W., "Microstructure, thermophysical and electrical properties in AlxCoCrFeNi (0≤x≤2) high-entropy alloys", Mater. Sci. Eng. B, 2009, 163, 184-189.

[8] Gao, M.C., Yeh, J.W., Liaw, P.K., Zhang, Y., "High-Entropy Alloys: Fundamentals and Applications", Springer, USA, 2016.

[9] Guo, S., Ng, C., Lu, J., Liu, C.T., "Effect of valence electron concentration on stability of FCC or BCC phase in high entropy alloys", J. Appl. Phys., 2011, 109, 503505.

[10] Ghasemi, A., Zamani, Kh., Tavoosi, M., Gordani, Gh.R., "Enhanced soft magnetic properties of CoNi-based high entropy alloys", J. Supercond. Nov. Magn., 2020, 33, 3189-3196.

[11] Zuo, T.T., Li, R.B., Ren, X.J., Zhang, Y., "Effects of Al and Si addition on the structure and properties of CoFeNi equal atomic ratio alloy", J. Magn. Magn. Mater., 2014, 371, 60-68.

[12] Xu, J., Axinte, E., Zhao, Z., Wang, Y., "Effect of C and Ce addition on the microstructure and magnetic property of the mechanically alloyed FeSiBAlNi high entropy alloys", J. Magn. Magn. Mater., 2016, 414, 59-68.

[13] Qiushi, C., Junjia, Z., Yiping, L., "Microstructure and Properties of AlCoCrFeNiB$_x$ (x= 0, 0.1, 0.25, 0.5, 0.75, 1.0) High Entropy Alloys", Rare Met. Mater. Eng., 2017, 46, 651-656.

[14] Qi, T., Li, Y., Takeuchi, A., Xie, G., Miao, H., "Soft magnetic Fe$_{25}$Co$_{25}$Ni$_{25}$(B, Si)$_{25}$ high entropy bulk metallic glasses", Intermetallics, 2015, 66, 8-12.

[15] Wei, R., Tao, J., Sun, H., Chen, C., Sun, G.W., "Soft magnetic Fe$_{26.7}$Co$_{26.7}$Ni$_{26.6}$Si$_9$B$_{11}$ high entropy metallic glass with good bending ductility", Mater. Lett., 2017, 197, 87-89.

[16] Li, Y., Zhang, W., Qi, T., "New soft magnetic Fe$_{25}$Co$_{25}$Ni$_{25}$(P, C, B)$_{25}$ high entropy bulk metallic glasses with large supercooled liquid region", J. Alloys Compd., 2017, 693, 25-31.

[17] Feng, W., Qi, Y., Wang, S.Q., "Effects of Mn and Al addition on structural and magnetic properties of FeCoNi-based high entropy alloys", Mater. Res. Exp., 2018, 5, 106511-106515.

[18] Li, P., Wang, A., Liu, C.T., "Composition dependence of structure, physical and mechanical properties of FeCoNi(MnAl)$_x$ high entropy alloys", Intermetallics, 2017, 87, 21-26.

[19] Zhang, K., Fu, Z., "Effects of annealing treatment on properties of CoCrFeNiTiAlx multi-component alloys", Intermetallics, 2012, 28, 34-39.

[20] Ma, S.G., Zhang, Y., "Effect of Nb addition on the microstructure and properties of AlCoCrFeNi high entropy alloy", Mater. Sci. Eng. A, 2012, 532, 480-486.

[21] Li, P., Wang, A., Liu, C.T., "A ductile high entropy alloy with attractive magnetic properties", J. Alloys Compd., 2017, 694, 55-60.

[22] Zhang, Y., Zuo, T.T., Cheng, Y.Q., "High entropy alloys with high saturation magnetization, electrical resistivity and malleability", Sci. Rep., 2013, 3, 1455-1461.

[23] Yu, P.F., Zhang, L.J., Chen, H., "The high entropy alloys with high hardness and soft magnetic property prepared by mechanical alloying and high pressure sintering", Intermetallics, 2016, 70, 82-87.

[24] Zuo, T.T., Gao, M.C., Ouyang, L., "Tailoring magnetic behavior of $CoFeMnNi_x$ (x= Al, Cr, Ga, and Sn) high entropy alloys by metal doping", Acta Mater., 2017, 130, 10-18.

[25] Yu, P.F., Zhang, L.J., Chen, H., "The high entropy alloys with high hardness and soft magnetic property prepared by mechanical alloying and high pressure sintering", Intermetallics, 2016, 70, 82-87.

[26] Lucas, M.S., Mauger, L., Munoz, J.A., "Magnetic and vibrational properties of high entropy alloys", J. App. Phy., 2011, 109, 07E307.

[27] Wang, X.F., Zhang, Y., Qiao, Y., "Novel microstructure and properties of multicomponent CoCrCuFeNiTix alloys", Intermetallics, 2007, 15, 357-362.

[28] Qiu, X.W., Zhang, Y.P., Liu, C.G., "Effect of Ti content on structure and properties of $Al_2CrFeNiCoCuTix$ high-entropy alloy coatings", J. Alloys Compd., 2014, 585, 282-286.